

# MAGNETIC COMPOSITES: MAGNONIC EXCITATIONS vs. THREE-DIMENSIONAL STRUCTURAL PERIODICITY

M. Krawczyk\* and H. Puzkarski

Surface Physics Division, Faculty of Physics, Adam Mickiewicz University,  
ul. Umultowska 85, 61-614 Poznań, Poland

## ABSTRACT

This study deals with the spin wave spectrum in magnetic macrostructure (composed of two ferromagnetic materials) showing a 3D periodicity: spherical ferromagnetic grains disposed in the nodes of a simple cubic crystal lattice are embedded in a matrix with different ferromagnetic properties. It is shown that the *magnonic spectrum* of this composite structure exhibits frequency regions *forbidden* for magnon propagation, and the energy gaps are found to be sensitive to the exchange contrast between the constituent materials as well as to the magnetization contrast. The widths of the respective magnonic gaps are studied as functions of parameters characterizing the magnetic structure.

**Keywords:** magnonic crystals, spin waves, periodic composites

**PACS numbers:** 75.50.-y; 75.30.Ds; 75.40.Gb

---

\*Corresponding author; e-mail: krawczyk@amu.edu.pl

# INTRODUCTION

Although the first study of electromagnetic wave propagation in periodic structures, written by Lord Rayleigh, was published already in 1887, it is only in recent years that photonic composites raised suddenly an extremely interest. The research in this field was initiated by the studies by Yablonovitch and John [1, 2] published in 1987 and anticipating the existence of complete energy gaps in electromagnetic wave spectra in three-dimensional periodic composites, henceforth referred to as *photonic crystals*. These can be used for fabricating new optoelectronic devices in which the role of electrons, traditionally used as transport medium, would be played by photons [3, 4, 5]. The so-called *left-handed materials* (LHM), showing negative effective refractivity [6, 7], provide an example of periodic materials demonstrating how much the properties of this kind of structure can differ from those of homogeneous materials. Another type of periodic composites are structures composed of materials with different *elastic* properties; showing an energy gap in their *elastic* wave spectrum, such composites are referred to as *phononic crystals* [8, 9, 10]. Recently, attention has been focused on the search of photonic and phononic crystals in which both the position and the width of the energy gap could be controlled by external factors, such as applied voltage or magnetic field. Attempts have been made to create photonic crystals in which one of the component materials is a magnetic [11, 12, 13, 14, 15, 16].

A magnetic periodic composite consists of at least two magnetic materials; the information carrier in such structures are spin waves. By analogy to photonic and phononic crystals, in which the role of information carrier is played by photons and phonons respectively, periodic magnetic composites are referred to as *magnonic crystals*. Studies of 2D magnonic crystals have been reported [17, 18, 19, 20, 22, 23], with scattering centers in the form of "infinitely" long cylinders disposed in square lattice nodes (cylinder and matrix materials being two different ferromagnetics), and the anticipated gaps were found indeed in the respective spin wave spectra. Further research was focused on magnetic multilayer systems, which can be regarded as 1D magnonic crystals [24, 25, 26, 27, 28, 29, 30, 31, 32].

In this paper, we present numerically calculated magnonic band structures of *three-dimensional* magnonic crystals. Due to the complexity of the problem, only the simplest model of 3D magnonic crystal is considered here, represented by a system of ferromagnetic spheres (which act as scattering centers) disposed in the nodes of a simple cubic crystal lattice and embedded in a different ferromagnetic material (matrix). Both the exchange and dipolar interactions are taken into account in our calculations based on the plane wave method and using the linear approximation.

## THEORY OF 3D MAGNONIC BAND STRUCTURE

Let's consider an ideal periodic structure consisting of spheres of ferromagnetic **A** and embedded in a matrix of ferromagnetic **B**. The spheres are assumed to form a 3D periodical lattice of *sc* type (Fig. 1a). A static magnetic field,  $H_0$ , is applied to the composite along the  $z$  axis, and assumed to be strong enough to saturate the magnetization of both materials. The lattice constant is denoted by  $a$ ; the filling fraction,  $f = 4/3\pi R^3 a^{-3}$ , is defined as the volume proportion of material **A** in a unit cell.

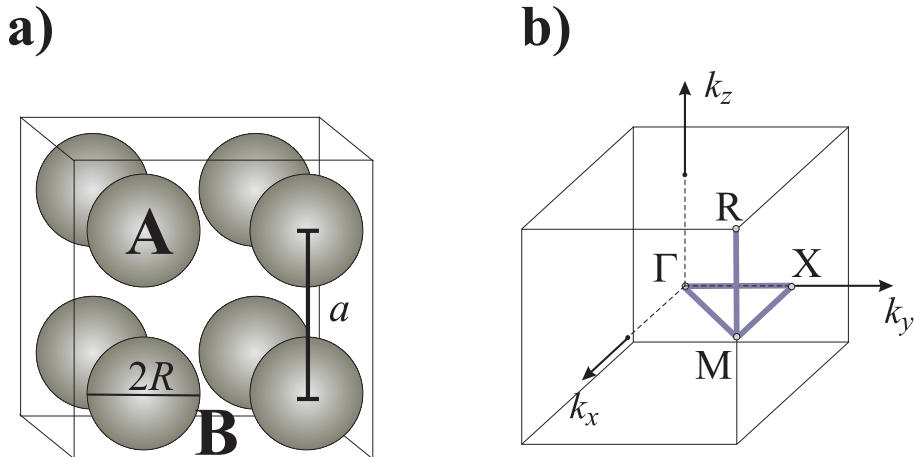


Figure 1: a) The 3D periodic structure studied in this paper; the structure consists of ferromagnetic spheres of material **A** embedded in a matrix of material **B** (materials **A** and **B** have different magnetic properties); the spheres are disposed in the nodes of a *sc* lattice. (b) The Brillouin zone corresponding to the considered structure, and the path  $M\Gamma XMR$  (highlighted) along which the magnonic band spectra are calculated.

Ferromagnetics **A** and **B** are characterized by two material parameters: the spontaneous

magnetization ( $M_{S,A}$  and  $M_{S,B}$ ), and the exchange constant ( $A_A$  and  $A_B$ ); both these parameters depend on the position vector  $\vec{r} = (x, y, z)$ :

$$\begin{aligned} M_S(\vec{r}) &= M_{S,B} + (M_{S,A} - M_{S,B})S(\vec{r}), \\ A(\vec{r}) &= A_B + (A_A - A_B)S(\vec{r}), \end{aligned} \quad (1)$$

the value of function  $S(\vec{r})$  being 1 inside a sphere, and 0 beyond.

In the classical approximation spin waves are described by the Landau-Lifshitz (LL) equation, taking the following form in the case of magnetic composites (with damping neglected):

$$\frac{\partial \vec{M}(\vec{r}, t)}{\partial t} = \gamma \mu_0 \vec{M}(\vec{r}, t) \times \vec{H}_{eff}(\vec{r}, t), \quad (2)$$

where magnetization  $\vec{M}(\vec{r}, t)$  is a function of position vector  $\vec{r}$  and time  $t$ ;  $\vec{H}_{eff}(\vec{r}, t)$  stands for the effective magnetic field [18, 19, 20, 21] acting on magnetization  $\vec{M}(\vec{r}, t)$ :

$$\vec{H}_{eff}(\vec{r}, t) = H_0 \hat{z} + \vec{h}(\vec{r}, t) + \frac{2}{\mu_0} \left( \nabla \cdot \frac{A}{M_S^2} \nabla \right) \vec{M}(\vec{r}, t); \quad (3)$$

$\hat{z}$  is the unit vector along the  $z$  axis;  $\vec{h}(\vec{r}, t)$  is the dynamic magnetic field due to dipolar interactions; the third component represents the exchange field. The magnetization vector can be represented as the sum of its static component,  $M_S \hat{z}$ , which is parallel to the applied field, and its dynamic component,  $\vec{m}(\vec{r}, t)$ , lying in plane  $(x, y)$ :

$$\vec{M}(\vec{r}, t) = M_S \hat{z} + \vec{m}(\vec{r}, t). \quad (4)$$

The dynamic dipolar field,  $\vec{h}$ , must satisfy the magnetostatic Maxwell equations:

$$\begin{aligned} \nabla \times \vec{h}(\vec{r}) &= 0, \\ \nabla \cdot (\vec{h}(\vec{r}) + \vec{m}(\vec{r})) &= 0. \end{aligned} \quad (5)$$

In a magnonic crystal, the position-dependent coefficients in (3), *i.e.*  $M_S$  and  $A$ , are periodic functions of the position vector, which allows us to use, in the procedure of solving the LL equation defined in (2), the plane wave method, described in detail in our

earlier papers [18, 19] (dealing with *two-dimensional* magnonic crystals). Following this scheme, we proceed to Fourier-expanding all the periodic functions of the position vector, *i.e.* the spontaneous magnetization,  $M_S$ , and parameter  $Q$  defined as follows:

$$Q = \frac{2A}{\mu_0 M_S^2 H_0}. \quad (6)$$

The dynamic components of the magnetization can be expressed as the product of the periodic envelope function and the Bloch factor  $\exp(i\vec{k}\vec{r})$  ( $\vec{k}$  denoting a 3D wave vector); the envelope function can be transformed into the reciprocal space as well. Including all the expansions into (2) and (5) leads to the following infinite system of linear equations for Fourier coefficients of the dynamic magnetization components,  $\vec{m}_{x\vec{k}}(\vec{G})$  and  $\vec{m}_{y\vec{k}}(\vec{G})$ :

$$\begin{aligned} i\Omega m_{x\vec{k}}(\vec{G}) &= m_{y\vec{k}}(\vec{G}) + \sum_{\vec{G}'} \frac{(k_y + G'_y)(k_x + G'_x)m_{x\vec{k}}(\vec{G}') + (k_y + G'_y)^2 m_{y\vec{k}}(\vec{G}')}{H_0 |\vec{k} + \vec{G}'|^2} M_S(\vec{G} - \vec{G}') \\ &\quad + \sum_{\vec{G}'} \sum_{\vec{G}''} [(\vec{k} + \vec{G}') \cdot (\vec{k} + \vec{G}'') - (\vec{G} - \vec{G}'') \cdot (\vec{G} - \vec{G}')] M_S(\vec{G} - \vec{G}'') Q(\vec{G}'' - \vec{G}') m_{y\vec{k}}(\vec{G}'), \\ i\Omega m_{y\vec{k}}(\vec{G}) &= -m_{x\vec{k}}(\vec{G}) - \sum_{\vec{G}'} \frac{(k_y + G'_y)(k_x + G'_x)m_{y\vec{k}}(\vec{G}') + (k_x + G'_x)^2 m_{x\vec{k}}(\vec{G}')}{H_0 |\vec{k} + \vec{G}'|^2} M_S(\vec{G} - \vec{G}') \\ &\quad - \sum_{\vec{G}'} \sum_{\vec{G}''} [(\vec{k} + \vec{G}') \cdot (\vec{k} + \vec{G}'') - (\vec{G} - \vec{G}'') \cdot (\vec{G} - \vec{G}')] M_S(\vec{G} - \vec{G}'') Q(\vec{G}'' - \vec{G}') m_{x\vec{k}}(\vec{G}'), \end{aligned} \quad (7)$$

$k_x, k_y$  and  $G_x, G_y$  denoting the Cartesian components of the wave vector  $\vec{k}$  and a reciprocal lattice vector  $\vec{G}$ , respectively; a new quantity introduced in (7) is  $\Omega$ , henceforth referred to as *reduced frequency*:

$$\Omega = \frac{\omega}{|\gamma| \mu_0 H_0}. \quad (8)$$

The Fourier coefficients of spontaneous magnetization  $M_S$  and parameter  $Q$  are calculated from the inverse Fourier transformation; in the case of spheres the resulting formulae read for  $M_S$  as follows:

$$M_S(\vec{G}) = \begin{cases} M_{S,A}f + M_{S,B}(1-f), & \text{for } \vec{G} = 0 \\ f(M_{S,A} - M_{S,B}) \frac{3[\sin(GR) - (GR)\cos(GR)]}{(GR)^3}, & \text{for } \vec{G} \neq 0 \end{cases}$$

and similarly for  $Q$ ;  $R$  is the sphere radius (Fig. 1a).

Obviously, the numerical calculations performed on the basis of (7) involve a finite number of reciprocal lattice vectors  $\vec{G}$  in the Fourier expansions; however, we have made sure that the number used is large enough to ensure good convergence of the numerical results. As indicated by an analysis performed, a satisfactory convergence is obtained already with 343 reciprocal lattice vectors used.

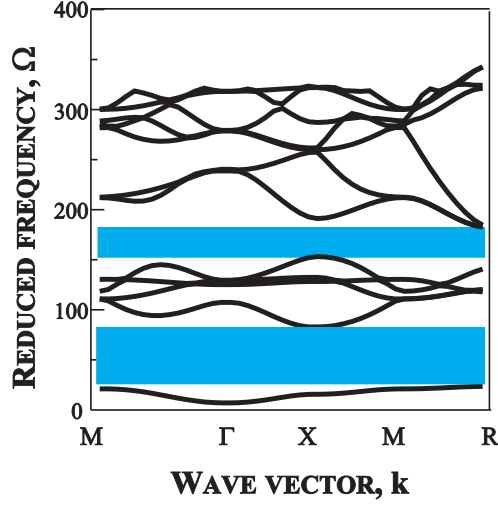


Figure 2: The magnonic band structure found numerically for the  $sc$  lattice-based composite (iron spheres embedded in a YIG matrix). The spin wave energy branches have been calculated along the path (in the first Brillouin zone) shown in Fig. 1b for the filling fraction  $f=0.2$ . The lattice constant value is assumed to be  $a = 100\text{\AA}$ , and the applied magnetic field value is  $\mu_0 H_0 = 0.1\text{T}$ .

## NUMERICAL RESULTS

The 3D magnonic crystal studied is a magnetic composite consisting of ferromagnetic spheres (of material **A**) disposed in the nodes of a  $sc$  lattice and embedded in a different magnetic material (**B**), referred to as matrix (Fig. 1). The corresponding magnonic band structure will be calculated along path  $M = \pi/a(1, 1, 0) \rightarrow \Gamma = \pi/a(0, 0, 0) \rightarrow X = \pi/a(0, 1, 0) \rightarrow M = \pi/a(1, 1, 0) \rightarrow R = \pi/a(1, 1, 1)$  in the nonreducible part of the first Brillouin zone (see Fig. 1). Iron (Fe) and yttrium iron garnet (YIG) are chosen as component materials **A** (spheres) and **B** (matrix), respectively, in the studied

example. As established in our earlier studies [18, 19] (in the case of 2D magnonic crystals) such composition, involving a substantial contrast of the magnetic parameters between the component materials ( $M_{S,Fe} = 1.752 \cdot 10^6 \text{ Am}^{-1}$ ,  $M_{S,YIG} = 0.194 \cdot 10^6 \text{ Am}^{-1}$ ,  $A_{Fe} = 2.1 \cdot 10^{-11} \text{ Jm}^{-1}$ ,  $A_{YIG} = 0.4 \cdot 10^{-11} \text{ Jm}^{-1}$ ), leads to opening large energy gaps in the spin wave spectrum. Also in the spin wave spectrum obtained for the *sc* lattice-based 3D magnonic crystal considered here, two wide energy gaps are present, one between bands 1 and 2, the other between bands 5 and 6, as shown in Fig. 2. The existence of the gap signifies that spin waves having frequency values within the gap cannot propagate through the composite. The following parameter values have been assumed in our calculations: crystal lattice constant  $a=100\text{\AA}$ , applied static magnetic field  $\mu_0 H_0 = 0.1\text{T}$ , and filling fraction  $f=0.2$ .

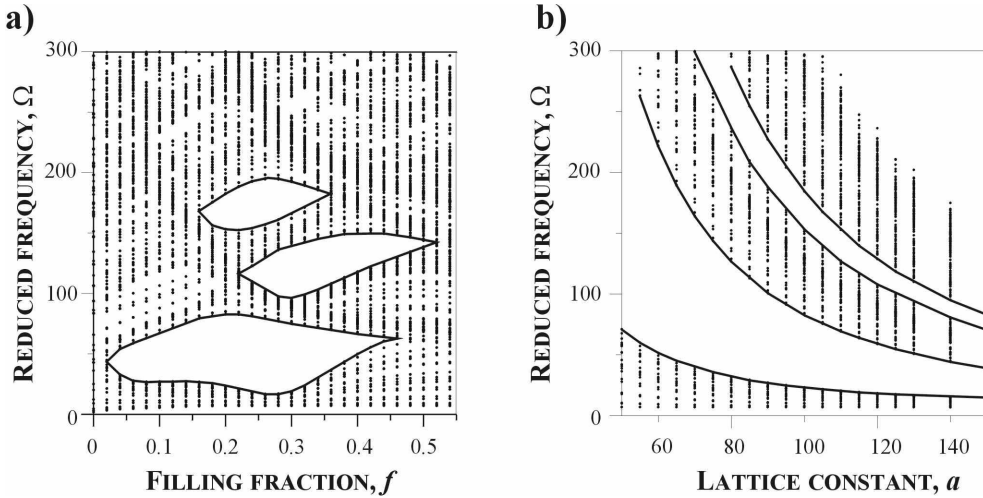


Figure 3: (a) The magnonic energy branches in the Fe/YIG simple cubic magnonic crystal plotted *versus* the filling fraction. The lattice constant value is assumed to be  $a = 100\text{\AA}$ , and the applied magnetic field value is  $\mu_0 H_0 = 0.1\text{T}$ . (b) Magnonic branches plotted versus the lattice constant  $a$  of the same *sc* structure; the filling fraction is fixed at  $f = 0.2$ . A frequency gap (the white region) moves down with increasing  $a$ .

Let's examine the effect of the filling fraction on the width of the spectral gaps. Figure 3a shows the magnonic bands plotted against the filling fraction in the *sc* lattice-based structure (*Fe* spheres embedded in YIG). The plot was obtained through projecting the magnonic band structure calculated along *MTXMR* path (for a fixed filling fraction

value) on the reduced frequency ( $\Omega$ ) axis; afterwards the procedure of projection was performed repeatedly for consecutive filling fraction values. The maximum width of the first gap is found to occur at  $f=0.27$ , reaching value  $\Delta\Omega=63.02$ . Unlike in 1D and 2D magnonic crystals [18, 19, 24], no oscillatory variations of the energy gaps with the filling fraction are observed in the considered 3D composite. Figure 3b shows the computed magnonic band structure plotted against the lattice constant  $a$  for  $f = 0.2$ . The gap center ( $\Omega_0$ ) is found to descend, and the gap itself  $\Delta\Omega$  (the white region) to narrow as the lattice constant increases, in such a way that the reduced gap width  $\Delta\Omega/\Omega_0$  remains almost constant.

Let's proceed now to the role played by magnetic parameters characterizing component materials. Figure 4a show spin wave energy branches plotted against the contrast between the spontaneous magnetization values in materials **A** (spheres) and **B** (matrix); this contrast, defined as ratio  $M_{S,A}/M_{S,B}$ , will be henceforth referred to as *magnetization contrast*. The computations have been performed for a fictitious matrix material whose spontaneous magnetization and exchange constant values,  $M_{S,B}$  and  $A_B$ , respectively, are fixed at values close to those in YIG; the exchange constant value in the sphere material is assumed to be  $A_A = 2.1 \cdot 10^{-11} Jm^{-1}$ . The other parameters are fixed as well: the lattice constant value is  $a=100\text{\AA}$ , the filling fraction  $f=0.2$ , and the applied magnetic field  $\mu_0 H_0 = 0.1T$ . It is seen that the gap width is maximal for the magnetization contrast value 13, which is not far from the magnetization contrast between iron and YIG ( $M_{S,Fe}/M_{S,YIG} = 10.82$ ); note also that the required value of magnetization contrast necessary for the energy gap to open is greater than 2.

We shall now examine the role of the contrast between the exchange constant values in the component materials. The results of the respective computations are depicted in Fig. 4b, showing magnonic branches *versus* the *exchange contrast*, defined as the ratio ( $A_A/A_B$ ) of exchange constant values in materials **A** (spheres) and **B** (matrix); the only variable in the computations was the exchange constant in material **A**. All other structural and

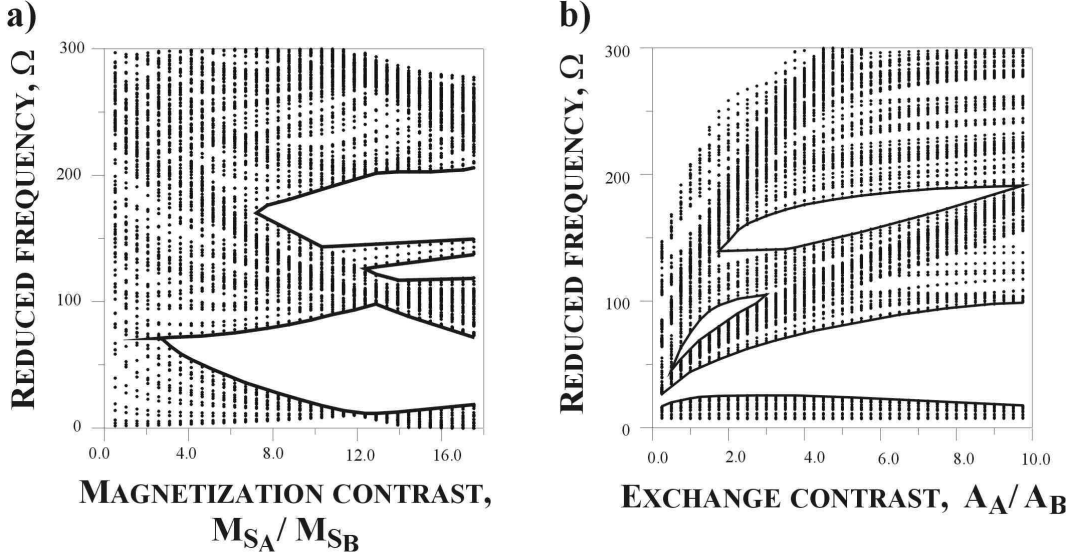


Figure 4: (a) Magnonic spectra plotted *versus* the magnetization contrast for a *sc* lattice-based structure. The exchange constant value in the spheres is assumed to be  $A_A = 2.1 \cdot 10^{-11} \text{Jm}^{-1}$ . (b) Magnonic branches plotted versus the exchange contrast; the spontaneous magnetization in the spheres is assumed to be  $M_{S,A} = 2.1 \cdot 10^6 \text{Am}^{-1}$ . The assumed spontaneous magnetization and exchange constant values of the matrix are:  $M_{S,B} = 0.194 \cdot 10^6 \text{Am}^{-1}$  and  $A_B = 0.4 \cdot 10^{-11} \text{Jm}^{-1}$ ; the lattice constant  $a = 100 \text{\AA}$ , the filling fraction  $f = 0.2$ , and the applied field  $\mu_0 H_0 = 0.1 \text{T}$ .

material parameters are fixed at the following values:  $M_{S,A} = 1.752 \cdot 10^6 \text{Am}^{-1}$ ,  $M_{S,B} = 0.194 \cdot 10^6 \text{Am}^{-1}$ ,  $A_B = 0.4 \cdot 10^{-11} \text{Jm}^{-1}$ ,  $a = 100 \text{\AA}$ ,  $\mu_0 H_0 = 0.1 \text{T}$ . From the Fig. 4b one can infer that the exchange contrast is not an indispensable factor for the opening of complete energy gaps in 3D magnonic crystals.

## CONCLUSIONS

We demonstrated that the 3D *magnonic crystal* with a *sc* lattice-based structure exhibits complete energy gaps, whose appearance is due to *two magnetic contrasts*: (1) the *exchange* contrast and (2) the *magnetization* contrast. Gaps are found to exist only when the spontaneous magnetization contrast is greater than 2. However, the gap width can be also controlled through adjusting the respective structural factors: the filling fraction value and the composite lattice constant.

## ACKNOWLEDGEMENT

The present work was supported by the Polish State Committee for Scientific Research through projects KBN - 2P03B 120 23 and PBZ-KBN-044/P03-2001.

## REFERENCES

- [1] E. Yablonovitch, Phys. Rev. Lett. **58** (1987) 2059.
- [2] S. John, Phys. Rev. Lett. **58** (1987) 2486.
- [3] *Development and Applications of Materials Exhibiting Photonic Gaps*, Eds. C. M. Bowden, J. P. Dowling, H. O. Everitt, J. Opt. Soc. Am. B **10** (1993) 280.
- [4] J. D. Joannopoulos, R. D. Meade, J. N. Winn, *Photonic Crystals*, Princeton Univ. Press, Princeton, NJ (1995).
- [5] K. Sakoda, *Optical Properties of Photonic Crystals*, Springer, Berlin (2001).
- [6] J. B. Pendry, Phys. Rev. Lett. **85** (2000) 3966.
- [7] J. B. Pendry, D. R. Smith, Physics Today **57** (June 2004) 37.
- [8] M. S. Kushwaha, P. Halevi, L. Dobrzynski, B. Djafari-Rouhani, Phys. Rev. Lett. **71** (1993) 2022.
- [9] M. M. Sigalas, E. N. Economou, Solid State Communications **86** (1993) 141.
- [10] Y. Lai, Z.-Q. Zhang, Appl. Phys. Lett. **83** (2003) 3900.
- [11] M. M. Sigalas, C. M. Soukoulis, R. Biswas, K. M. Ho, Phys. Rev. B **56** (1997) 959.
- [12] A. Saib, D. Vanhoenacker-Janvier, I. Huynen, A. Encinas, L. Piraux, E. Ferain, R. Legras, Appl. Phys. Lett. **83** (2003) 2378.
- [13] Z. Lin, S. T. Chui, Phys. Rev. E **69** (2004) 056614.

- [14] P. Xu, T.-Y. Cai, Z.-Y. Li, Solid State Communications **130** (2004) 451.
- [15] S.A. Nikitov, Ph. Tailhades, Optics Communications **199** (2001) 389.
- [16] I.L. Lyubchanskii, N.N. Dadoenkova, M.I. Lyubchanskii, E.A. Shapovalov and T. Rasing, J. Phys. D: Appl. Phys. **36** (2003) R277.
- [17] J. O. Vasseur, L. Dobrzynski, B. Djafari-Rouhani, H. Puzzkarski, Phys. Rev. B **54** (1996) 1043.
- [18] M. Krawczyk, H. Puzzkarski, Acta Physica Polonica A **93** (1998) 805.
- [19] M. Krawczyk, H. Puzzkarski, Acta Physicae Superficierum **3** (1999) 89.
- [20] H. Puzzkarski, M. Krawczyk, Solid State Phenomena **94** (2003) 125.
- [21] L.D. Landau and E.M. Lifshitz, Phys. Z. Sowjetunion **8** (1935) 153.
- [22] Y.V. Gulyaev, S.A. Nikitov, L.V. Zhivotovskii, A.A Klimov, P. Tailhades, L. Presmanes, C. Bonningue, C.S. Tsai, S.L. Vysotskii, Y.A.Filimonov, J.E.T.P. Letters **77** (2003) 670.
- [23] M. Shamonin, A. Snarskii and M. Zhenirovskiy, NDT&E International **37** (2004) 35.
- [24] A. Akjouj, A. Mir, B. Djafari-Rouhani, J.O. Vasseur, L. Dobrzynski, H. Al Wahsh, P.A. Deymier, Surface Science **482** (2001) 1062.
- [25] A. Mir, H. Al Wahsh, A. Akjouj, B. Djafari-Rouhani, L. Dobrzynski, J.O. Vasseur, J. Phys.: Condens. Matter **14** (2002) 637.
- [26] H. Puzzkarski, M. Krawczyk, Physics Letters A **282** (2001) 106.
- [27] H. Puzzkarski, M. Krawczyk, J.-C. S. Levy, D. Mercier, Acta Physica Polonica A **100** (Supplement) (2001) 195.

- [28] S.A. Nikitov, Ph. Tailhades, C.S. Tsai, J. Magn. Magn. Mater. **236** (2001) 320.
- [29] H. Al-Wahsh, Phys. Rev. B **69** (2004) 012405.
- [30] V.V. Kruglyak, A.N. Kuchko, The Physics of Metals and Metallography **93** (2002) 511.
- [31] V.V. Kruglyak, A.N. Kuchko, Physica B **339** (2003) 130.
- [32] V.V. Kruglyak, A.N. Kuchko, J. Magn. Magn. Mater. **272-276** (2004) 302.